CHAPTER 4.

1-Year (2013), 3-Year (2011–13), and 5-Year (2009–13) Drought Maps for the Conterminous United States

Frank H. Koch
John W. Coulston

INTRODUCTION

Droughts occur regularly in most U.S. forests, but their frequency and intensity vary widely between, as well as within, forest ecosystems (Hanson and Weltzin 2000). In the Western United States, forests commonly experience annual seasonal droughts. In the Eastern United States, forests tend to exhibit one of two prevailing drought patterns: random (i.e., occurring at any time of year), occasional droughts, as typically seen in the Appalachian Mountains and the Northeast; or frequent late-summer droughts, as typically seen in the southeastern Coastal Plain and the eastern edge of the Great Plains (Hanson and Weltzin 2000).

Initially, plants respond to drought stress by decreasing fundamental growth processes such as cell division and enlargement. Photosynthesis, which is less sensitive than these basic processes, decreases slowly when drought stress is low, but more sharply when the stress is moderate to severe (Kareiva and others 1993, Mattson and Haack 1987). Drought stress often makes forests susceptible to attack by tree-damaging insects and diseases (Clinton and others 1993, Mattson and Haack 1987, Raffa and others 2008). Moreover, drought increases wildland fire risk by inhibiting organic matter decomposition and diminishing the moisture content of downed woody materials and other potential fire fuels (Clark 1989, Keetch and Byram 1968, Schoennagel and others 2004).

Forests are generally resistant to short-term drought conditions (Archaux and Wolters 2006), although individual tree species have differing degrees of resistance (Hinckley and others 1979, McDowell and others 2008). Because of this resistance, the duration of a drought event may be more important than its intensity (Archaux and Wolters 2006); for instance, multiple consecutive years of drought (2 to 5 years) are more likely to cause high tree mortality than a single very dry year (Guarín and Taylor 2005, Millar and others 2007). Therefore, a comprehensive account of drought impact in forested areas should include analysis of moisture conditions over multiyear time windows.

In the 2010 Forest Health Monitoring (FHM) national report, we presented a methodology for mapping drought conditions across the conterminous United States (Koch and others 2013a). Our goal with this methodology was to generate drought-related spatial data sets that are finer in scale than similar products available from sources such as the National Climatic Data Center (2015) or the U.S. Drought Monitor Program (Svoboda and others 2002). The principal inputs are gridded climate data (i.e., monthly raster maps of precipitation and temperature over a 100-year period) created with the Parameter-elevation Regression on Independent Slopes (PRISM) climate mapping system (Daly and others 2002). Notably, the methodology employs a standardized drought-indexing approach that allows us to compare a given location's moisture status during different time windows, regardless of their length. Our drought index is easier to calculate than the commonly used Palmer Drought Severity Index, or PDSI (Palmer

1965), and sidesteps some criticisms of the PDSI (summarized by Alley 1984) regarding its underlying assumptions and limited comparability across space and time. In this chapter, we apply the methodology to the most currently available climate data (i.e., the monthly PRISM data through 2013), thereby providing a fifth time step in an ongoing annual record of drought status in the conterminous United States from 2009 forward (Koch and others 2013a, 2013b, 2014, 2015).

METHODS

We acquired grids for monthly precipitation and monthly mean temperature for the conterminous United States from the PRISM Climate Group Web site (PRISM Climate Group 2014). At the time of these analyses, gridded data sets were available for all years from 1895 to 2013. However, the grids for December 2013 were only provisional versions (i.e., finalized grids had not yet been released for this month). For analytical purposes, we treated these provisional grids as if they were the final versions. The spatial resolution of the grids was approximately 4 km (cell area = 16 km^2). For future applications and to ensure better compatibility with other spatial data sets, all output grids were resampled to a spatial resolution of approximately 2 km (cell area = 4 km^2) using a nearest neighbor approach. The nearest neighbor approach is a computationally simple resampling method that avoids the smoothing of data values observed with methods such as bilinear interpolation or cubic convolution.

Potential Evapotranspiration Maps

As in our previous drought mapping efforts (Koch and others 2012a, 2012b, 2013a, 2013b, 2014, 2015), we adopted an approach in which a moisture index value for each location of interest (i.e., each grid cell in a map of the conterminous United States) was calculated based on both precipitation and potential evapotranspiration values for that location during the time period of interest. Potential evapotranspiration measures the loss of soil moisture through plant uptake and transpiration (Akin 1991). It does not measure actual moisture loss, but rather the loss that would occur if there was no possible shortage of moisture for plants to transpire (Akin 1991, Thornthwaite 1948). The inclusion of both precipitation and potential evapotranspiration provides a fuller accounting of a location's water balance than precipitation alone.

To complement the available PRISM monthly precipitation grids, we computed corresponding monthly potential evapotranspiration (*PET*) grids using Thornthwaite's formula (Akin 1991, Thornthwaite 1948):

$$PET_m = 1.6 L_{lm} (10 \frac{T_m}{I})^a \qquad (1)$$

where

PET_m = the potential evapotranspiration for a given month *m* in cm

L_{lm} = a correction factor for the mean possible duration of sunlight during month *m* for all locations (i.e., grid cells) at a particular latitude l [see table V in Thornthwaite (1948) for a list of L correction factors by month and latitude]

T_m = the mean temperature for month m in degrees C

I = an annual heat index, calculated as

$$I = \sum_{m=1}^{12} \left(\frac{T_m}{5} \right)^{1.514}$$

where

T_m = the mean temperature for each month m of the year

a = an exponent calculated as $a = 6.75 \times 10^{-7} I^3 - 7.71 \times 10^{-5} I^2 + 1.792 \times 10^{-2} I + 0.49239$ [see appendix I in Thornthwaite (1948) regarding calculation of I and the empirical derivation of a]

Although only a simple approximation, a key advantage of Thornthwaite's formula is that it has modest input data requirements (i.e., mean temperature values) compared to more sophisticated methods of estimating *PET* such as the Penman-Monteith equation (Monteith 1965), which requires less readily available data on factors such as humidity, radiation, and wind speed. To implement equation 1 spatially, we created a grid of latitude values for determining the L adjustment for any given grid cell (and any given month) in the conterminous United States. We extracted the T_m values for the grid cells from the corresponding PRISM mean monthly temperature grids.

Moisture Index Maps

To estimate baseline conditions, we used the precipitation (*P*) and *PET* grids to generate moisture index grids for the past 100 years (i.e., 1914–2013) for the conterminous United States. We used a moisture index described by Willmott and Feddema (1992), which has been applied in a variety of contexts, including global vegetation modeling (Potter and Klooster 1999) and climate change analysis (Grundstein 2009). Willmott and Feddema (1992) devised the index as a refinement of one described earlier by Thornthwaite (1948) and Thornthwaite and Mather (1955). Their revised index, *MI'*, has the following form:

$$MI' = \begin{cases} P/PET - 1 & , \quad P < PET \\ 1 - PET/P & , \quad P \geq PET \\ 0 & , \quad P = PET = 0 \end{cases} \qquad (2)$$

where

P = precipitation

PET = potential evapotranspiration

(*P* and *PET* must be in equivalent measurement units, e.g., mm)

This set of equations yields a symmetric, dimensionless index scaled between -1 and 1. *MI'* can be calculated for any time period, but is commonly calculated on an annual basis using summed *P* and *PET* values (Willmott and Feddema 1992). An alternative to this summation approach is to calculate *MI'* from monthly precipitation and potential evapotranspiration values and then, for a given time window of interest, calculate its moisture index as the mean of the *MI′* values for all months in the time window. This "mean-of-months" approach limits the ability of short-term peaks in either precipitation or potential evapotranspiration to negate corresponding short-term deficits, as would happen under a summation approach.

For each year in our study period (i.e., 1914–2013), we used the mean-of-months approach to calculate moisture index grids for three different time windows: 1 year (MI_1'), 3 years (MI_3'), and 5 years (MI_5'). Briefly, the MI_1' grids are the mean of the 12 monthly *MI′* grids for each year in the study period, the MI_3' grids are the mean of the 36 monthly grids from January two years prior through December of the target year, and the MI_5' grids are the mean of the 60 consecutive monthly *MI′* grids from January four years prior to December of the target year. For example, the MI_1' grid for the year 2013 is the mean of the monthly *MI′* grids from January through December 2013, while the MI_3' grid is the mean of the grids from January 2011 through December 2013 and the MI_5' grid is the mean of the grids from January 2009 through December 2013.

ANNUAL AND MULTIYEAR DROUGHT MAPS

To determine degree of departure from typical moisture conditions, we first created a normal grid, $MI'_{i\ norm}$, for each of our three time windows, representing the mean of the 100 corresponding moisture index grids (i.e., the MI_1', MI_3', or MI_5' grids, depending on the window; see fig. 4.1). We also created a standard deviation grid, $MI'_{i\ SD}$, for each time window, calculated from the window's 100 individual moisture index grids as well as its $MI'_{i\ norm}$ grid. We subsequently calculated moisture difference *z*-scores, MDZ_{ij}, for each time window using these derived data sets:

$$MDZ_{ij} = \frac{MI_i' - MI'_{i\ norm}}{MI'_{i\ SD}} \tag{3}$$

where

i = the analytical time window (i.e., 1, 3, or 5 years)

j = a particular target year in our 100-year study period (i.e., 1914–2013)

MDZ scores may be classified in terms of degree of moisture deficit or surplus (table 4.1). The classification scheme includes categories (e.g., severe drought, extreme drought) like those associated with the PDSI. The scheme has also been adopted for other drought indices such as the Standardized Precipitation Index, or SPI (McKee and others 1993). Moreover, the breakpoints between *MDZ* categories resemble those used for the SPI, such that we expect the *MDZ* categories to have theoretical frequencies of occurrence that are similar to their SPI counterparts (e.g., approximately 2.3 percent of the time for extreme drought; see McKee and others 1993, Steinemann 2003). More importantly, because of the standardization in equation 3, the breakpoints between categories

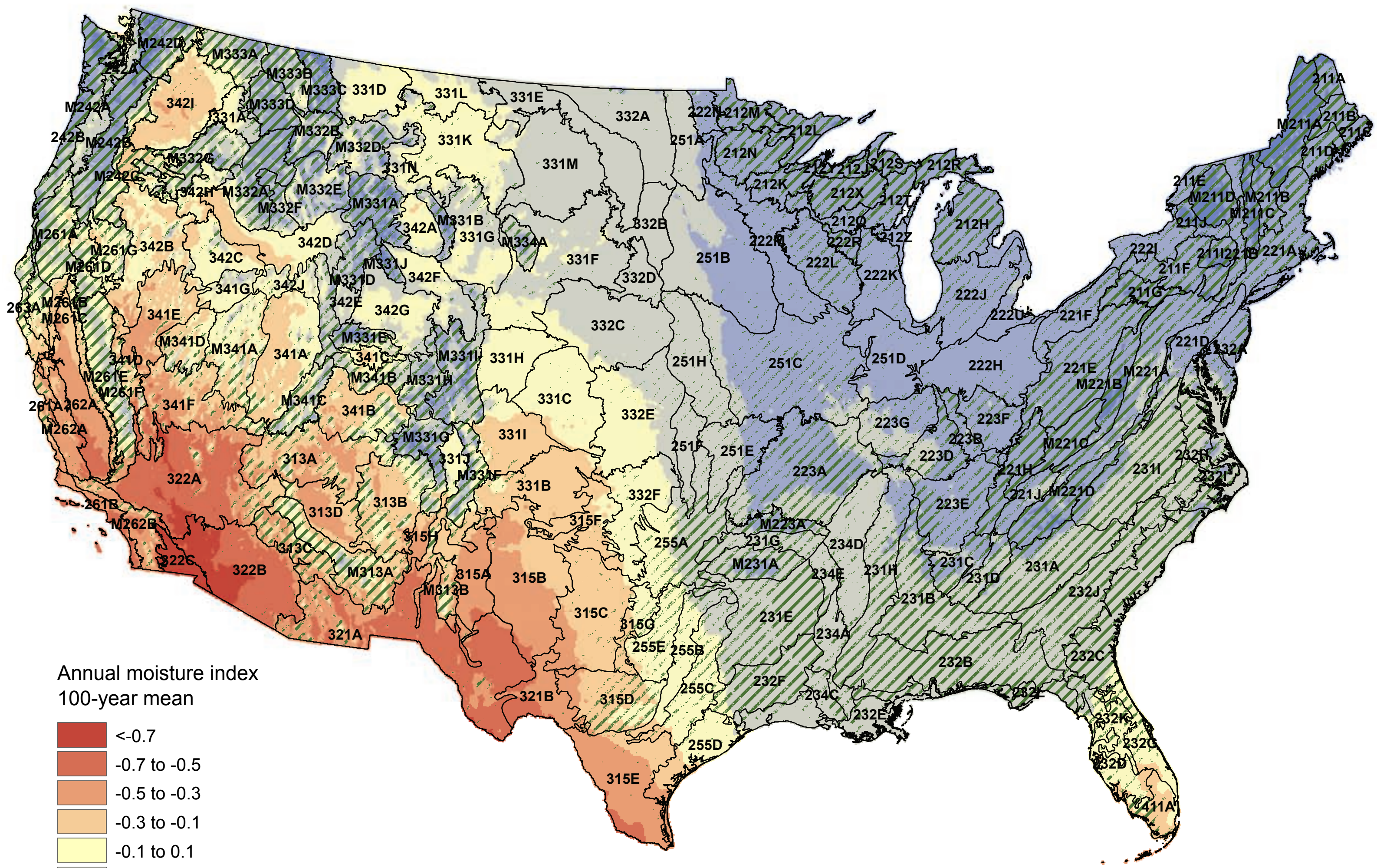

Figure 4.1—The 100-year (1914–2013) mean annual moisture index, or $MI'_{1\ norm}$*, for the conterminous United States. Ecoregion section (Cleland and others 2007) boundaries and labels are included for reference. Forest cover data (overlaid green hatching) derived from Moderate Resolution Imaging Spectroradiometer (MODIS) imagery by the U.S. Department of Agriculture Forest Service, Remote Sensing Applications Center. (Data source: PRISM Climate Group, Oregon State University)*

Table 4.1—Moisture difference *z*-score (*MDZ*) value ranges for nine wetness and drought categories, along with each category's approximate theoretical frequency of occurrence

MDZ score	Category	Frequency
		percent
<-2	Extreme drought	2.3
-2 to -1.5	Severe drought	4.4
-1.5 to -1	Moderate drought	9.2
-1 to -0.5	Mild drought	15.0
-0.5 to 0.5	Near normal conditions	38.2
0.5 to 1	Mild moisture surplus	15.0
1 to 1.5	Moderate moisture surplus	9.2
1.5 to 2	Severe moisture surplus	4.4
>2	Extreme moisture surplus	2.3

remain the same regardless of the size of the time window of interest. For comparative analysis, we generated classified *MDZ* maps of the conterminous United States, based on all three time windows, for the target year 2013. Because our analysis focused on drought (i.e., moisture deficit) rather than surplus conditions, we combined the four moisture surplus categories from table 4.1 into a single category for map display.

RESULTS AND DISCUSSION

The 100-year (1914–2013) mean annual moisture index, or $MI_{1}'{}_{norm}$, grid (fig. 4.1) provides an overview of climatic regimes in the conterminous United States. (The 100-year $MI_{3}'{}_{norm}$ and $MI_{5}'{}_{norm}$ grids did not differ substantially from the mean $MI_{1}'{}_{norm}$ grid, and are not shown here.) Wet climates ($MI' > 0$) are common in the Eastern United States, particularly the Northeast. A noteworthy anomaly is southern Florida, especially ecoregion sections 232G–Florida Coastal Lowlands-Atlantic, 232D–Florida Coastal Lowlands-Gulf, and 411A–Everglades. This region appears to be dry relative to other parts of the East. Although southern Florida usually receives a high level of precipitation over the course of a year, this is countered by a high level of potential evapotranspiration, which results in negative *MI′* values. This is fundamentally different from the pattern observed in the driest parts of the Western United States, especially the Southwest (e.g., sections 322A–Mojave Desert, 322B–Sonoran Desert, and 322C–Colorado Desert), where potential evapotranspiration is very high but precipitation levels are very low. In fact, dry climates ($MI' < 0$) are typical across much of the Western United States because of generally lower precipitation than the East. Nevertheless, mountainous areas in the central and northern Rocky Mountains as well as the Pacific Northwest are relatively wet, such as ecoregion sections M242A–Oregon and Washington Coast Ranges, M242B–Western Cascades, M331G–South-Central Highlands, and M333C–Northern Rockies. This may be driven in part by large amounts of winter snowfall in these regions.

Figure 4.2 shows the annual (i.e., 1-year) *MDZ* map for 2013 for the conterminous United States. Much of the country experienced moisture surplus conditions during the year. The southern portion of the Pacific Coast was a prominent exception, as most ecoregion

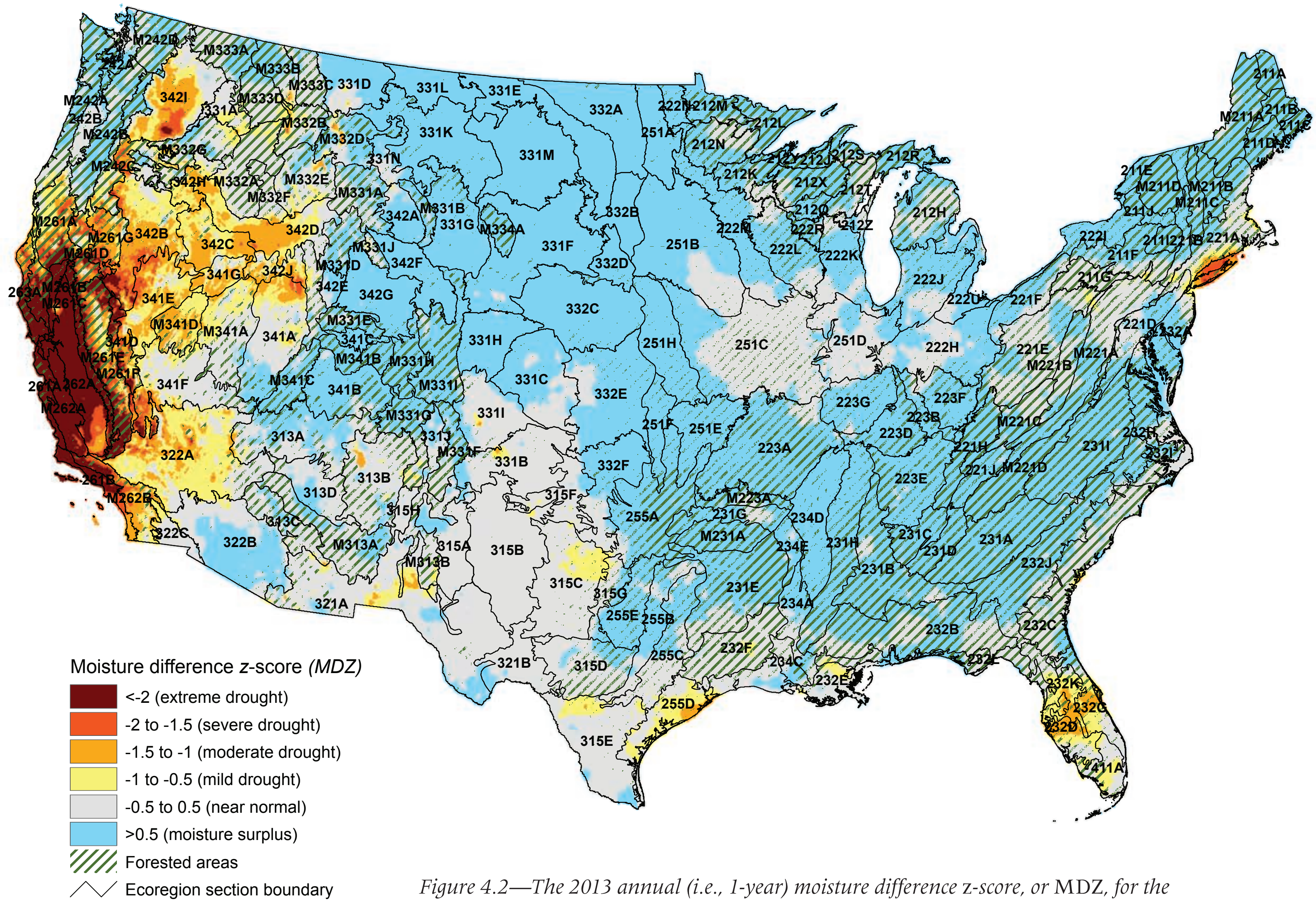

Figure 4.2—The 2013 annual (i.e., 1-year) moisture difference z-score, or MDZ, for the conterminous United States. Ecoregion section (Cleland and others 2007) boundaries and labels are included for reference. Forest cover data (overlaid green hatching) derived from MODIS imagery by the U.S. Department of Agriculture Forest Service, Remote Sensing Applications Center. (Data source: PRISM Climate Group, Oregon State University)

sections (Cleland and others 2007) falling at least partially within the State of California experienced extreme drought conditions (*MDZ* < -2) in 2013. Forested sections in this region that contained sizeable areas of extreme drought included M261A–Klamath Mountains, M261B–Northern California Coast Ranges, M261E–Sierra Nevada, M262B–Southern California Mountain and Valley, 263A–Northern California Coast, and 341D–Mono. In addition, extreme drought conditions extended across all of section 261A–Central California Coast and nearly all of M261F–Sierra Nevada Foothills. Furthermore, other forested sections in this region, such as M261D–Southern Cascades and M261G–Modoc Plateau, were subjected to moderate or worse drought conditions (*MDZ* < -1) during 2013. Moderate or worse drought conditions also occurred in portions of neighboring geographic regions (i.e., the Pacific Northwest and the Intermountain West), but were typically limited to areas with little or no forest; the only ecoregion sections where moderate or worse drought conditions and substantial forest cover coincided were M341D–West Great Basin and Mountains and the western portion of 342H–Blue Mountain Foothills.

Although droughts have been common throughout the West during recent decades (Andreadis and Lettenmaier 2006, Andreadis and others 2005, Groisman and Knight 2008), the conditions in California in 2013 were unusually severe. It was the State's driest calendar year in the historical record, which began in 1895 (National Climatic Data Center 2014b). The city of San Francisco received only 142 mm of precipitation over the course of the year, while Los Angeles received only 91 mm (National Climatic Data Center 2014c). These amounts represented 24 percent of each city's normal annual precipitation.

The conditions in California and adjacent regions are especially striking because so few geographic hot spots of moderate or worse drought conditions appeared elsewhere in forested portions of the United States. Two hot spots worth mentioning are an area of moderate drought in central Florida, extending across sections 232G–Florida Coastal Lowlands-Atlantic, 232D–Florida Coastal Lowlands-Gulf, and 232K–Florida Coastal Plains Central Highlands, as well as an area of moderate to extreme drought in section 221A–Lower New England, primarily along New York's Long Island and the Connecticut coast. On balance, 2013 was a wet year relative to historical data. The percentage of the conterminous United States with moderate or worse drought conditions based on the Palmer Drought Severity Index reached a low of 13.4 percent in October, but increased somewhat to 18.5 percent by the end of December (National Climatic Data Center 2014b).

Figure 4.3 shows a map of the change in *MDZ* category between 2012 and 2013 for the conterminous United States. The depicted increases and decreases reference the *MDZ* categories listed in table 4.1. As was the case

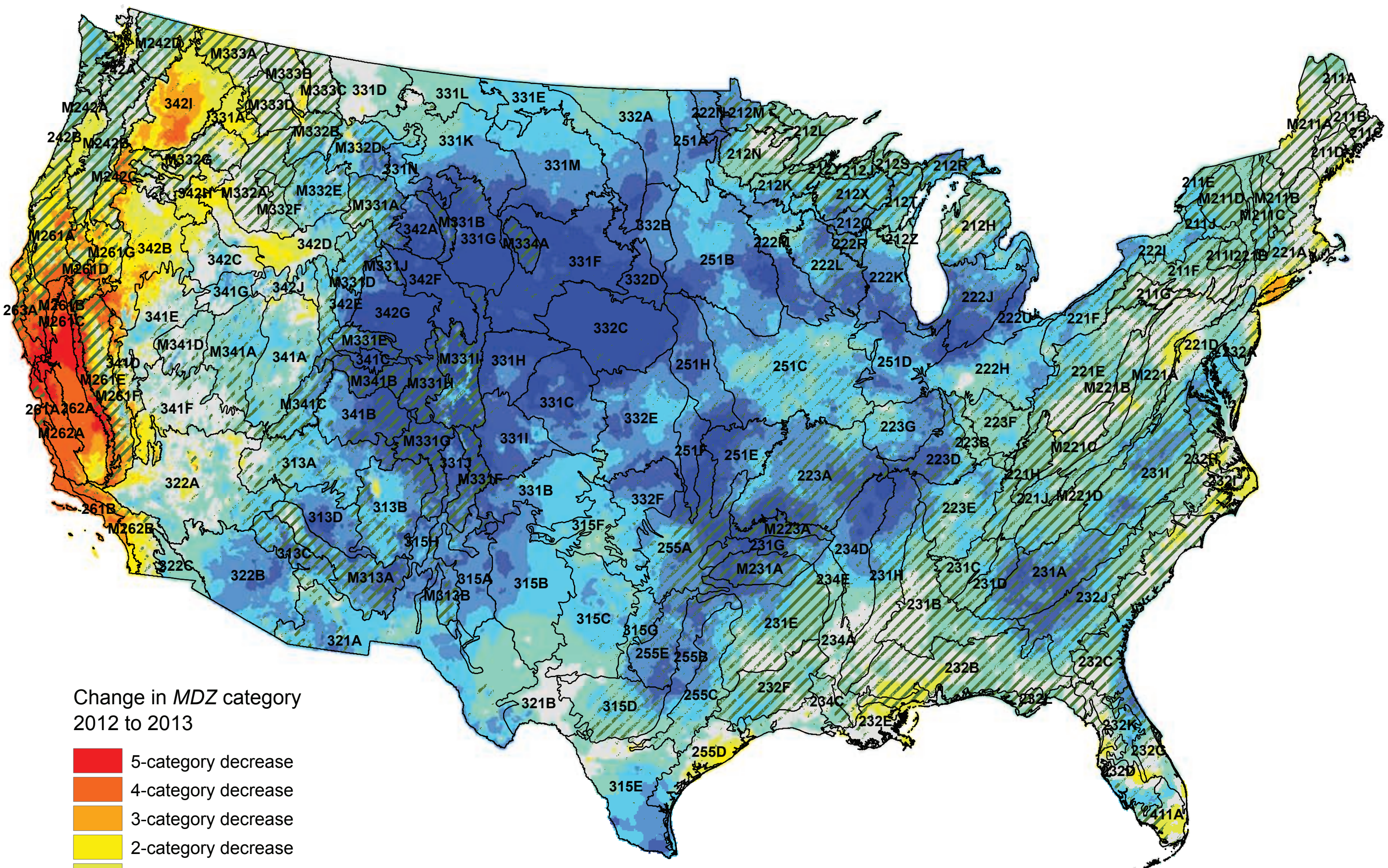

Figure 4.3—Change in moisture difference z-score (MDZ) *category between 2012 and 2013. See table 1 for a list of the* MDZ *categories used in this analysis; a five-category decrease indicates a change from moisture surplus in 2012 to extreme drought in 2013, while a five-category increase indicates a change from extreme drought in 2012 to moisture surplus in 2013. Ecoregion section (Cleland and others 2007) boundaries and labels are included for reference. Forest cover data (overlaid green hatching) derived from MODIS imagery by the U.S. Department of Agriculture Forest Service, Remote Sensing Applications Center. (Data source: PRISM Climate Group, Oregon State University)*

for figure 4.2, all of the moisture surplus categories in table 4.1 have been combined into a single category, yielding a six-point scale from extreme drought to moisture surplus. Thus, a five-category decrease indicates a change from moisture surplus in 2012 to extreme drought in 2013, while a five-category increase indicates a change from extreme drought to moisture surplus. The other map classes depict less extreme changes between years. For instance, a two-category decrease represents one of four possibilities: a change from moisture surplus to mild drought, from near-normal conditions to moderate drought, from mild to severe drought, or from moderate drought in 2012 to extreme drought in 2013.

Most of the conterminous United States displayed an increase in *MDZ* from 2012 to 2013 (fig. 4.3). In the Central United States, several large, contiguous areas exhibited a four- or five-category increase in *MDZ*, indicating widespread recovery from drought conditions between 2012 and 2013. Forested ecoregion sections that were in these contiguous areas included M331B–Bighorn Mountains, M331H–North Central Highlands and Rocky Mountains, M334A–Black Hills, M341B–Tavaputs Plateau, and several others. In contrast, the four- or five-category decrease in *MDZ* exhibited by most ecoregion sections in California indicates that the severe drought conditions observed in 2013 were preceded by near-normal or surplus moisture conditions throughout much of the State in 2012.

The 3-year (2011–13) (fig. 4.4) and 5-year (2009–13) (fig. 4.5) *MDZ* maps document the recent history of moisture conditions in the conterminous United States. Both maps, but especially the 3-year map (fig. 4.4), reflect some impact from the drought conditions that occurred in California in 2013. More broadly, the maps also suggest that drought conditions have persisted throughout the Southwestern United States for the last several years; both maps display extensive areas of severe to extreme drought (*MDZ* < -1.5) in this region. Indeed, intense and widespread droughts have occurred regularly in the Southwest for more than two decades (Groisman and Knight 2008; Mueller and others 2005; National Climatic Data Center 2010, 2011). The most severe multiyear drought conditions appear to have occurred in areas with little forest cover (e.g., 313D–Painted Desert, 331I–Arkansas Tablelands, and 341E–Northern Mono), but there are notable counter-examples, such as M313B–Sacramento-Monzano Mountains.

Elsewhere, both maps show a large area of extreme drought along the Gulf of Mexico coast in Texas and Louisiana, particularly in the heavily forested ecoregion section 232F–Coastal Plains and Flatwoods-Western Gulf. Both States were historically dry in 2011 and had record heat waves during the summer of that year (National Climatic Data Center 2012). A modest reduction in the area of extreme drought shown in the 3-year map (fig. 4.4) versus the 5-year map (fig. 4.5) indicates that moisture conditions improved

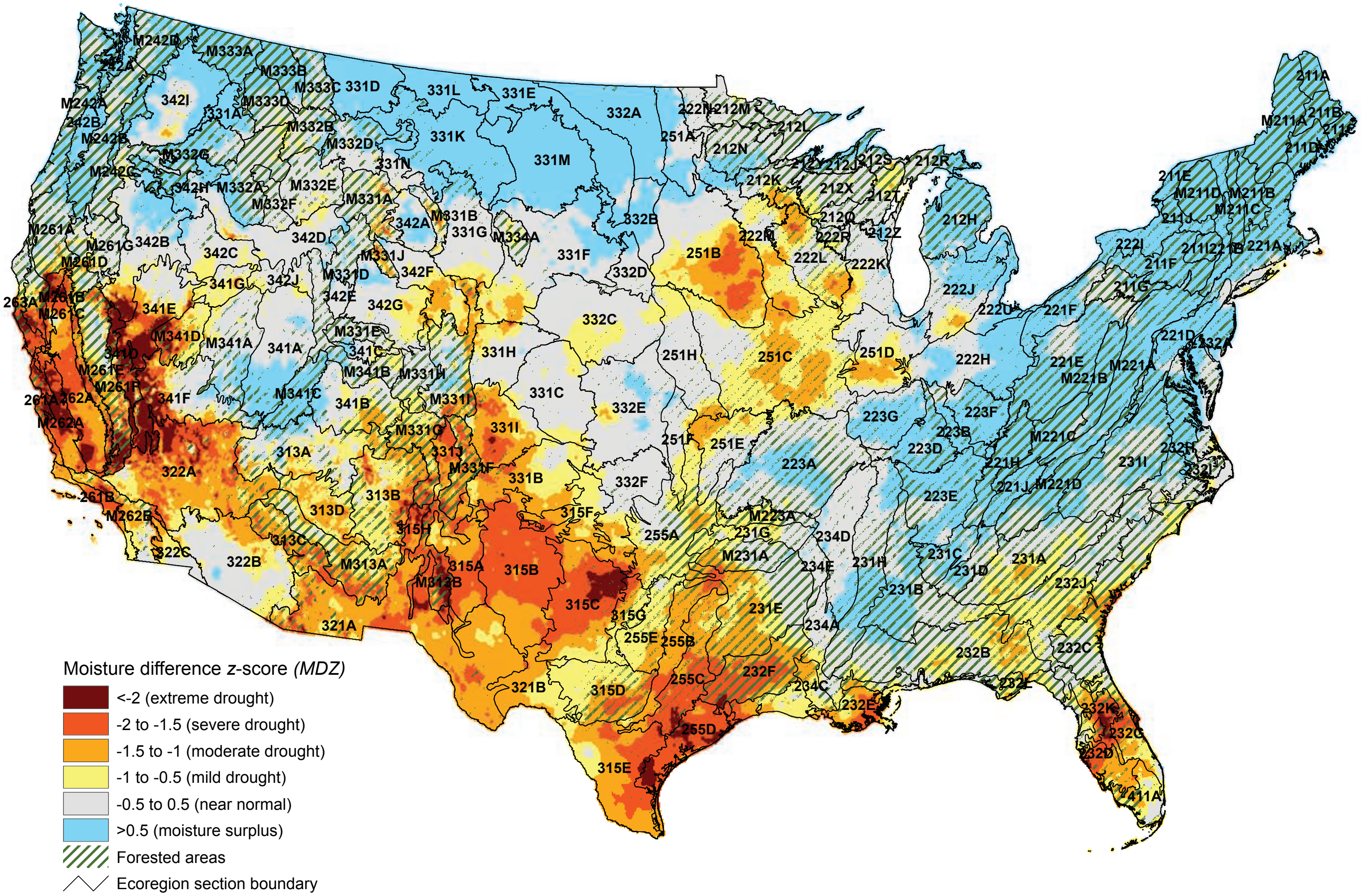

Figure 4.4—The 2011–13 (i.e., 3-year) moisture difference z-score (MDZ) *for the conterminous United States. Ecoregion section (Cleland and others 2007) boundaries are included for reference. Forest cover data (overlaid green hatching) derived from MODIS imagery by the U.S. Department of Agriculture Forest Service, Remote Sensing Applications Center. (Data source: PRISM Climate Group, Oregon State University)*

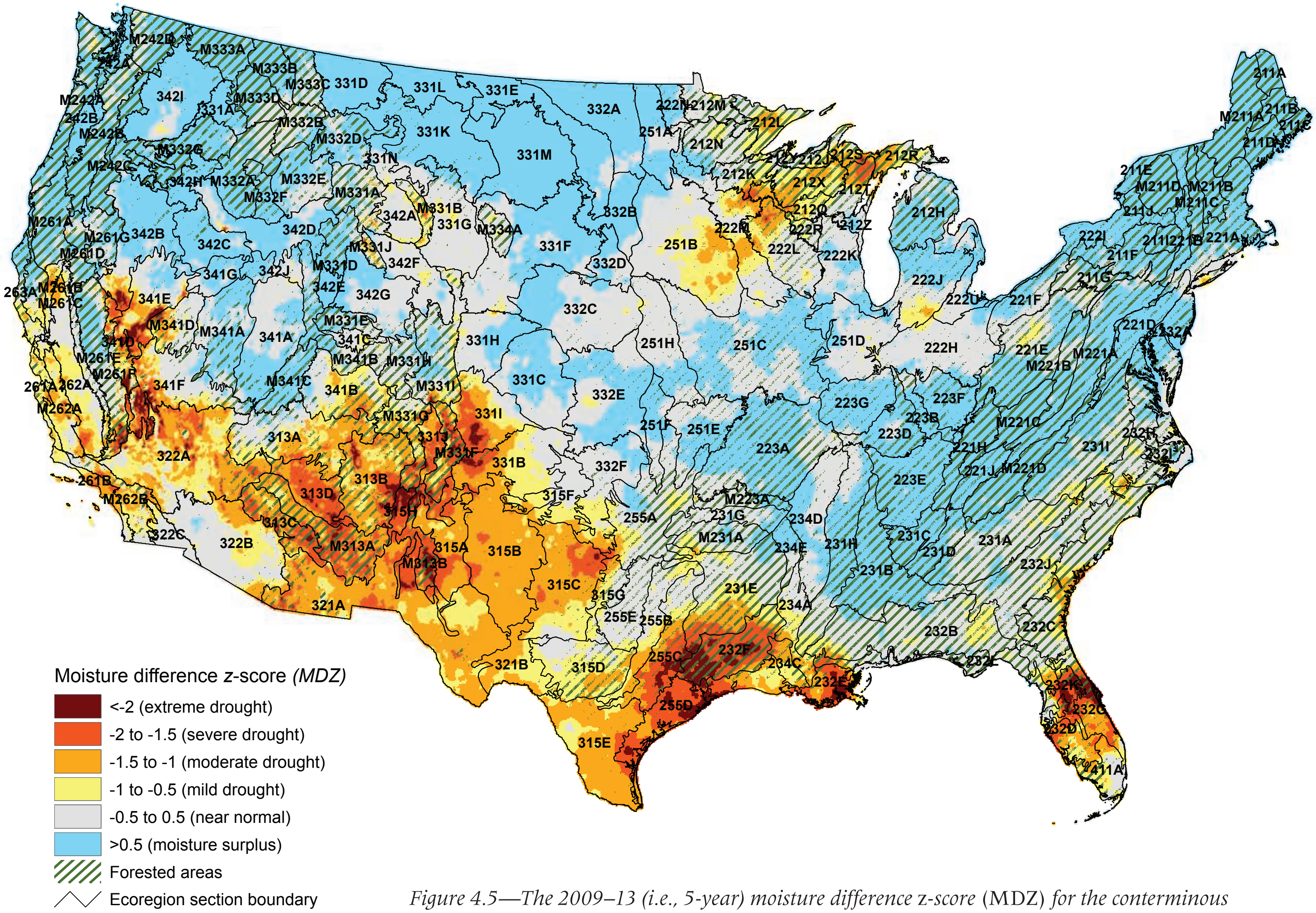

Figure 4.5—The 2009–13 (i.e., 5-year) moisture difference z-score (MDZ) *for the conterminous United States. Ecoregion section (Cleland and others 2007) boundaries are included for reference. Forest cover data (overlaid green hatching) derived from MODIS imagery by the U.S. Department of Agriculture Forest Service, Remote Sensing Applications Center. (Data source: PRISM Climate Group, Oregon State University)*

in this region during 2012 and 2013. This improvement is partially captured in the 1-year *MDZ* map for 2013 (fig. 4.2).

The hot spot of moderate drought in central Florida that appeared in the 1-year *MDZ* map also appeared in the 3- and 5-year maps, but with higher levels of drought severity. Drought conditions also extended over a larger area of the State in the multiyear maps. This seems consistent with the historical record; according to long-term climatological rankings (National Climatic Data Center 2014a), the period from July 2010 to June 2011 was Florida's driest 12-month period to date (i.e., since 1895). In contrast, although Florida experienced somewhat dry conditions at the beginning and end of 2013, this was countered by historically wet conditions during June and July.

Future Efforts

If the appropriate spatial data (i.e., high-resolution maps of precipitation and temperature) remain available for public use, we will continue to produce our 1-year, 3-year, and 5-year *MDZ* maps of the conterminous United States as a regular yearly component of national-scale forest health reporting. However, users should interpret and compare the *MDZ* drought maps presented here cautiously. Although the maps use a standardized index scale that applies regardless of the size of the time window, the window size may still merit some consideration; for example, an extreme drought that persists over a 5-year period has substantially different forest health implications than an extreme drought over a 1-year period. Furthermore, while the 1-year, 3-year, and 5-year *MDZ* maps may together provide a comprehensive short-term overview, it may also be important to consider a particular region's longer term drought history when assessing the current health of its forests. For example, in geographic regions where droughts have historically occurred on a frequent (e.g., annual or nearly annual) basis, certain tree species may be better adapted to a regular lack of available moisture (McDowell and others 2008). Because of this variability in species' drought tolerance, a long period of persistent and severe drought conditions could ultimately lead to changes in a region's forest composition (Mueller and others 2005). In future work, we hope to provide forest managers and other decisionmakers with better quantitative evidence regarding critical relationships between drought and significant forest health impacts such as regional-scale tree mortality (e.g., Mitchell and others 2014). We also intend to examine the role of drought as an inciting factor for other forest threats such as wildfire or pest outbreaks.

LITERATURE CITED

Akin, W.E. 1991. Global patterns: climate, vegetation, and soils. Norman, OK: University of Oklahoma Press. 370 p.

Alley, W.M. 1984. The Palmer Drought Severity Index: limitations and assumptions. Journal of Climate and Applied Meteorology. 23: 1100-1109.

Andreadis, K.M.; Clark, E.A.; Wood, A.W. [and others]. 2005. Twentieth-century drought in the conterminous United States. Journal of Hydrometeorology. 6: 985-1001.

Andreadis, K.M.; Lettenmaier, D.P. 2006. Trends in 20th century drought over the continental United States. Geophysical Research Letters. 33(10): L10403.

Archaux, F.; Wolters, V. 2006. Impact of summer drought on forest biodiversity: what do we know? Annals of Forest Science. 63: 645-652.

Clark, J.S. 1989. Effects of long-term water balances on fire regime, north-western Minnesota. Journal of Ecology. 77: 989-1004.

Cleland, D.T.; Freeouf, J.A.; Keys, J.E., Jr. [and others]. 2007. Ecological subregions: sections and subsections for the conterminous United States. In: Sloan, A.M., tech. ed. Gen. Tech. Rep. WO–76. Washington, DC: U.S. Department of Agriculture Forest Service. [Map, presentation scale 1:3,500,000; Albers equal area projection; colored]. [Also available as a Geographic Information System coverage in ArcINFO® format on CD-ROM or online at http://data.fs.usda.gov/geodata/edw/datasets.php. [Date accessed: July 20, 2015].

Clinton, B.D.; Boring, L.R.; Swank, W.T. 1993. Canopy gap characteristics and drought influences in oak forests of the Coweeta Basin. Ecology. 74(5): 1551-1558.

Daly, C.; Gibson, W.P.; Taylor, G.H. [and others]. 2002. A knowledge-based approach to the statistical mapping of climate. Climate Research. 22: 99-113.

Groisman, P.Y.; Knight, R.W. 2008. Prolonged dry episodes over the conterminous United States: new tendencies emerging during the last 40 years. Journal of Climate. 21: 1850-1862.

Grundstein, A. 2009. Evaluation of climate change over the continental United States using a moisture index. Climatic Change. 93: 103-115.

Guarín, A.; Taylor, A.H. 2005. Drought triggered tree mortality in mixed conifer forests in Yosemite National Park, California, USA. Forest Ecology and Management. 218: 229-244.

Hanson, P.J.; Weltzin, J.F. 2000. Drought disturbance from climate change: response of United States forests. The Science of the Total Environment. 262: 205-220.

Hinckley, T.M.; Dougherty, P.M.; Lassoie, J.P. [and others]. 1979. A severe drought: impact on tree growth, phenology, net photosynthetic rate, and water relations. American Midland Naturalist. 102(2): 307-316.

Kareiva, P.M.; Kingsolver, J.G.; Huey, B.B., eds. 1993. Biotic interactions and global change. Sunderland, MA: Sinauer Associates, Inc. 559 p.

Keetch, J.J.; Byram, G.M. 1968. A drought index for forest fire control. Res. Pap. SE–38. Asheville, NC: U.S. Department of Agriculture Forest Service, Southeastern Forest Experiment Station. 33 p.

Koch, F.H.; Coulston, J.W.; Smith, W.D. 2012a. High-resolution mapping of drought conditions. In: Potter, K.M.; Conkling, B.L., eds. Forest Health Monitoring 2008 national technical report. Gen. Tech. Rep. SRS–158. Asheville, NC: U.S. Department of Agriculture Forest Service, Southern Research Station: 45-62.

Koch, F.H.; Coulston, J.W.; Smith, W.D. 2012b. Mapping drought conditions using multi-year windows. In: Potter, K.M.; Conkling, B.L., eds. Forest Health Monitoring 2009 national technical report. Gen. Tech. Rep. SRS–167. Asheville, NC: U.S. Department of Agriculture Forest Service, Southern Research Station: 163-179.

Koch, F.H.; Smith, W.D.; Coulston, J.W. 2013a. An improved method for standardized mapping of drought conditions. In: Potter, K.M.; Conkling, B.L., eds. Forest Health Monitoring: national status, trends, and analysis 2010. SRS–176. Asheville, NC: U.S. Department of Agriculture Forest Service, Southern Research Station: 67-83.

Koch, F.H.; Smith, W.D.; Coulston, J.W. 2013b. Recent drought conditions in the conterminous United States. In: Potter, K.M.; Conkling, B.L., eds. Forest Health Monitoring: national status, trends, and analysis 2011. Gen. Tech. Rep. SRS–185. Asheville, NC: U.S. Department of Agriculture Forest Service, Southern Research Station: 41-48.

Koch, F.H.; Smith, W.D.; Coulston, J.W. 2014. Drought patterns in the conterminous United States and Hawaii. In: Potter, K.M.; Conkling, B.L., eds. Forest Health Monitoring: national status, trends, and analysis 2012. Gen. Tech. Rep. SRS–198. Asheville, NC: U.S. Department of Agriculture Forest Service Southern Research Station: 49-72.

Koch, F.H.; Smith, W.D.; Coulston, J.W. 2015. Drought patterns in the conterminous United States, 2012. In: Potter, K.M.; Conkling, B.L., eds. Forest Health Monitoring: national status, trends, and analysis 2013. Gen. Tech. Rep. SRS-207. Asheville, NC: U.S. Department of Agriculture Forest Service, Southern Research Station: 55-69.

Mattson, W.J.; Haack, R.A. 1987. The role of drought in outbreaks of plant-eating insects. BioScience. 37(2): 110-118.

McDowell, N.; Pockman, W.T.; Allen, C.D. [and others]. 2008. Mechanisms of plant survival and mortality during drought: why do some plants survive while others succumb to drought? New Phytologist. 178: 719-739.

McKee, T.B.; Doesken, N.J.; Kleist, J. 1993. The relationship of drought frequency and duration to time scales. In: Proceedings of the eighth conference on applied climatology. Boston, MA: American Meteorological Society: 179-184.

Millar, C.I.; Westfall, R.D.; Delany, D.L. 2007. Response of high-elevation limber pine *(Pinus flexilis)* to multiyear droughts and 20th-century warming, Sierra Nevada, California, USA. Canadian Journal of Forest Research. 37: 2508-2520.

Mitchell, P.J.; O'Grady, A.P.; Hayes, K.R.; Pinkard, E.A. 2014. Exposure of trees to drought-induced die-off is defined by a common climatic threshold across different vegetation types. Ecology and Evolution. 4(7): 1088-1101.

Monteith, J.L. 1965. Evaporation and environment. Symposia of the Society for Experimental Biology. 19: 205-234.

Mueller, R.C.; Scudder, C.M.; Porter, M.E. [and others]. 2005. Differential tree mortality in response to severe drought: evidence for long-term vegetation shifts. Journal of Ecology. 93: 1085-1093.

National Climatic Data Center. 2010. State of the climate - drought - annual report 2009. http://www.ncdc.noaa.gov/sotc/2009/13. [Date accessed: May 12, 2011].

National Climatic Data Center. 2011. State of the climate - drought - annual report 2010. http://www.ncdc.noaa.gov/sotc/drought/2010/13. [Date accessed: May 10, 2011].

National Climatic Data Center. 2012. State of the climate - drought - annual report 2011. http://www.ncdc.noaa.gov/sotc/drought/2011/13. [Date accessed: April 26, 2012].

National Climatic Data Center. 2014a. Climatological rankings - temperature, precipitation, and drought. http://www.ncdc.noaa.gov/temp-and-precip/climatological-rankings/index.php. [Date accessed: July 23, 2014].

National Climatic Data Center. 2014b. State of the climate - drought - annual report 2013. http://www.ncdc.noaa.gov/sotc/drought/2013/13. [Date accessed: July 18, 2014].

National Climatic Data Center. 2014c. State of the climate - drought - December 2013. http://www.ncdc.noaa.gov/sotc/drought/2013/12. [Date accessed: July 18, 2014].

National Climatic Data Center. 2015. Divisional temperature-precipitation-drought. Documentation for the nClimDiv database. U.S. Department of Commerce, National Oceanic and Atmospheric Administration, National Environmental Satellite, Data and Information Service, National Climatic Data Center. ftp://ftp.ncdc.noaa.gov/pub/data/cirs/climdiv/divisional-readme.txt. [Date accessed: March 26, 2015].

Palmer, W.C. 1965. Meteorological drought. Res. Pap. No. 45. Washington, DC: U.S. Department of Commerce Weather Bureau. 58 p.

Potter, C.S.; Klooster, S.A. 1999. Dynamic global vegetation modelling for prediction of plant functional types and biogenic trace gas fluxes. Global Ecology and Biogeography. 8(6): 473-488.

PRISM Climate Group. 2014. 2.5-arcmin (4 km) gridded monthly climate data. http://www.prism.oregonstate.edu. [Date accessed: June 9, 2014].

Raffa, K.F.; Aukema, B.H.; Bentz, B.J. [and others]. 2008. Cross-scale drivers of natural disturbances prone to anthropogenic amplification: the dynamics of bark beetle eruptions. BioScience. 58(6): 501-517.

Schoennagel, T.; Veblen, T.T.; Romme, W.H. 2004. The interaction of fire, fuels, and climate across Rocky Mountain forests. BioScience. 54(7): 661-676.

Steinemann, A. 2003. Drought indicators and triggers: a stochastic approach to evaluation. Journal of the American Water Resources Association. 39(5): 1217-1233.

Svoboda, M.; LeComte, D.; Hayes, M. [and others]. 2002. The drought monitor. Bulletin of the American Meteorological Society. 83(8): 1181-1190.

Thornthwaite, C.W. 1948. An approach towards a rational classification of climate. Geographical Review. 38(1): 55-94.

Thornthwaite, C.W.; Mather, J.R. 1955. The water balance. Publications in Climatology. 8(1): 1-104.

Willmott, C.J.; Feddema, J.J. 1992. A more rational climatic moisture index. Professional Geographer. 44(1): 84-87.